Pergamon

Bioorganic & Medicinal Chemistry 9 (2001) 3173–3183

BIOORGANIC & MEDICINAL CHEMISTRY

Conformationally Restricted PACAP27 Analogues Incorporating Type II/II′ IBTM β-Turn Mimetics. Synthesis, NMR Structure Determination, and Binding Affinity

Rosario González-Muñiz,[a,*] Mercedes Martín-Martínez,[a] Cesare Granata,[b,†] Eliandre de Oliveira,[b] Clara M. Santiveri,[c] Carlos González,[c] Diana Frechilla,[d] Rosario Herranz,[a] M. Teresa García-López,[a] Joaquín Del Río,[d] M. Angeles Jiménez[c] and David Andreu[b]

[a]*Instituto de Química Médica (CSIC), Juan de la Cierva 3, 28006 Madrid, Spain*
[b]*Departament de Química Orgànica, Universitat de Barcelona, Martí i Franqués 1-11, 08028 Barcelona, Spain*
[c]*Instituto de Estructura de la Materia (CSIC), Serrano 119, 28006 Madrid, Spain*
[d]*Departamento de Farmacología, Universidad de Navarra, Irunlarrea 1, 31008 Pamplona, Spain*

Received 17 January 2001; accepted 22 May 2001

Abstract—To probe the importance of a proposed β-turn within residues S9-R12 of PACAP for recognition by VIP/PACAP receptors, compounds **1** and **2**, two conformationally restricted analogues of PACAP27 incorporating respectively (*S*)- or (*R*)-IBTM as type II or II′ β-turn dipeptide mimetic at the Y10-S11 position, were synthesized. According to ^{1}H NMR conformational analyses in aqueous solution and 30% TFE, both PACAP27 and the [*S*-IBTM^{10,11}]PACAP27 analogue **1** adopt similar ordered structures. PACAP27 shows an N-terminal disordered region (residues H1-F6) and an α-helical conformation within segment T7–L27. For residues S9–R12, our data seem more compatible with a segment of the α-helix than with the β-turn previously proposed for this fragment. In compound **1** the α-helix, also spanning T7–L27 residues, appears slightly distorted at the N-terminus relative to the native peptide. Although this distortion could lead to the marked decrease in binding affinity of this compound at the VIP/PACAP receptors, the lack of the Y10 side chain in analogues **1** and **2** could also significantly affect the binding of these compounds.

Introduction

Pituitary adenylate cyclase-activating polypeptide (PACAP) is a member of the superfamily of regulatory peptides including secretin, glucagon, vasoactive intestinal polypeptide (VIP) and GRF.[1] PACAP exists in two bioactive C-terminally amidated forms, PACAP38 and its shortened N-terminal version, PACAP27. These polypeptides exert their actions through specific interaction with three classes of receptors: the PAC_1 receptor, which displays much higher affinity for the two forms of PACAP (IC_{50}, 1 nM) than for VIP (IC_{50}, 1000 nM), and the $VPAC_1$ and $VPAC_2$ receptors, that recognize PACAP38, PACAP27 and VIP with similar affinity, in the nanomolar range.[2] PACAP has been implicated in a broad range of biological processes including reproduction, growth, cardiovascular, respiratory and digestive functions, and immune responses.[1,3] There is also clear evidence that PACAP exerts trophic effects on different cell types and has protective properties on neuronal cell death induced by excitotoxins and other cellular injuries.[4–10] Despite the potential clinical interest of PACAP, there are few systematic studies in which the contribution of individual residues or peptide fragments to biological activity is evaluated. Selective peptide agonists and antagonists for the VIP/PACAP receptors include VIP/GRF hybrids,[11–13] cyclic peptides,[14,15] maxadilan and derivatives,[16,17] and VIP/PACAP fragments.[18,19] However, there is still a need for specific potent VIP/PACAP agonists and antagonists, most preferably peptidomimetics, for overcoming the known drawbacks of peptides as drugs. Better characterization of the three-dimensional conformation of PACAP could be an important goal for the design of

*Corresponding author. Fax: +34-1-564-4853; e-mail: iqmg313@iqm.csic.es
†Present address: Roche Discovery, Welwyn, Hertfordshire, UK.

0968-0896/01/$ - see front matter
PII: S0968-0896(01)00190-0

non-peptide VIP/PACAP receptor ligands. Two different structures in solution have been proposed for PACAP27. In the presence of trifluoroethanol (TFE), it has been described that PACAP27 has a disordered N-terminal domain followed by an α-helical stretch from residues S9 to V26, with a discontinuity between residues K20 and K21.[20] In 25% MeOH, the conformation of PACAP27 is composed of three distinct regions: a type II β-turn at residues S9–R12, and two α-helices spanning residues R12–K20 and Y22–A24.[21] Compared to VIP in the same solvent,[22] PACAP27 displays distinct conformational properties, regarding position and shape of the helix and the possibility of a unique β-turn-like conformation at residues S9–R12. Since minor conformational changes between PACAP and VIP are likely to contribute to the selective recognition of the receptors, increasing the rigidity of these peptides by incorporation of well-defined secondary structure motifs could constitute a first step in the design of peptidomimetic analogues.[23] Based on our previous experience in β-turn mimetics, we synthesized the conformationally restricted PACAP analogue **1**, in which the proposed β-turn at the S9–R12 region is fixed by replacement of the Y10–S11 dipeptide with *S*-IBTM, an efficient type II β-turn mimetic.[24–26] This paper deals with the synthesis, conformational study and binding affinities of [*S*-IBTM^{10,11}]PACAP27 (**1**),[27] in comparison with PACAP27. In order to evaluate the effect of the type of β-turn on binding affinity, analogue **2**, incorporating the type II' β-turn mimetic *R*-IBTM, was also prepared.

Results and Discussion

Chemistry

The synthesis of PACAP27 and its two analogues, **1** and **2**, was carried out by solid phase methods[28] using Boc/benzyl chemistry on *p*-methylbenzhydrylamine resin, with in situ neutralization[29] and DCC-mediated couplings (see Experimental for details). Previous evidence of sluggish incorporation of the Boc-*S*- or *R*-IBTM pseudodipeptides suggested the use of a powerful carboxyl activator such as HATU,[30] which indeed afforded practically quantitative coupling of either unit. The presence of dipeptide sequences likely to form aspartimides (D3–G4 and D8–S9 in PACAP27, and the first one in either **1** or **2**) and of an oxidation-prone Met residue made it advisable to deprotect and cleave the peptides from the resin by low-high HF[31] acidolysis. This proved to be a sound choice, providing in all cases a fairly clean crude in which the target sequence was identified as the major component by MALDI-TOF MS. These spectra showed a small peak at M-18, still present in apparently homogeneous fractions isolated after preparative HPLC. The suspected presence of an aspartimide contaminant in the HPLC-purified peptides was confirmed by capillary electrophoresis, which showed small (<8%) levels of a faster-eluting impurity in all three peptides. The aspartimide byproducts were effectively removed by isoelectrofocusing, followed by desalting (RP-HPLC). Overall yields (synthesis, acidolysis and purification) were in the 5% range.

NMR conformational study of PACAP27 and [*S*-IBTM^{10,11}]-PACAP27 (1)

The structure adopted by PACAP27 and its analogue **1** in aqueous solution and in 30% TFE was investigated by analysis of several NMR parameters, NOE connectivities and ^{1}H chemical shifts (δ). Tables 1 and 2 list the δ values. The strongest evidence comes from the NOE correlations, in particular from the non-sequential ones. The deviations of the CαH δ values observed in a given peptide relative to those expected for non-structured peptides [$\Delta\delta_{C\alpha H} = \delta_{C\alpha H(observed)} - \delta_{C\alpha H(randomcoil)}$] also provide information on peptide conformation, negative values being characteristic of α-helices and positive ones of β-sheets.[32–34] In aqueous solution, the negative $\Delta\delta_{C\alpha H}$ values, large in absolute value, observed for PACAP27 and for its analogue **1** (Fig. 1) indicated the presence of a helical structure spanning residues T7–L27 in the two peptides. In the case of peptide **1**, we cannot include the $\Delta\delta_{C\alpha H}$ values for residues 10 and 11 due to the lack of random coil reference value for the [*S*-IBTM^{10,11}] peptidomimetic. The few non-sequential NOEs that could be unambiguously identified for the two peptides in aqueous solution were all compatible with a helix structure (Fig. 1). The small number of observed non-sequential NOEs was probably due to

PACAP27 HSDGIFTDSY^{10}S^{11}RYRKQMAVKKYLAAVL–NH$_2$

[*S*-IBTM^{10,11}]PACAP27 (**1**) HSDGIFTDS[*S*-IBTM^{10,11}]RYRKQMAVKKYLAAVL–NH$_2$

[*R*-IBTM^{10,11}]PACAP27 (**2**) HSDGIFTDS[*R*-IBTM^{10,11}]RYRKQMAVKKYLAAVL–NH$_2$

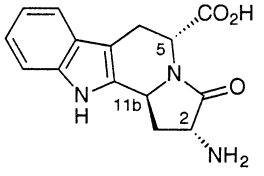

S-IBTM

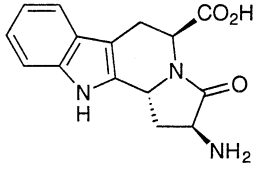

R-IBTM

Table 1. ^{1}H chemical shifts of PACAP27 and [*S*-IBTM^{10,11}]PACAP27 (in italics) in aqueous solution (H_2O/D_2O 9:1) at pH 3.5 and 5 °C (ppm, from TSP)

Residue	NH	$C_\alpha H$	$C_\beta H$	Others
H1		4.33	3.43, 3.37	$C_{\delta 2}H$ 7.41 $C_{\varepsilon 1}H$ 8.67
		4.35	*3.43, 3.38*	*7.41 8.68*
S2	8.93	4.57	3.87, 3.84	
	8.96	*4.57*	*3.89, 3.84*	
D3	8.86	4.74	2.84, 2.73	
	8.93	*4.79*	*2.90, 2.81*	
G4	8.48	3.89, 3.89		
	8.47	*3.87, 3.87*		
I5	8.04	4.08	1.74	$C_\gamma H$ 1.23,1.03 $C_\gamma H_3$ 0.75
	8.05	*4.07*	*1.67*	*1.19,0.99 0.60*
				$C_\delta H_3$ 0.77
				0.73
F6	8.57	4.74	3.17, 3.00	$C_\delta H$ 7.23, 7.23 $C_\varepsilon H$ 7.31,7.31
	8.52	*4.82*	*3.05, 2.89*	*6.88, 6.88 6.92,6.92*
				$C_\zeta H$ 7.28
				7.05
T7	8.19	4.28	4.21	$C_\gamma H$ 1.17
	8.43	*4.32*	*4.21*	*1.04*
D8	8.51	4.63	2.78, 2.78	
	8.81	*4.66*	*2.93, 2.85*	
S9	8.45	4.27	3.83, 3.83	
	8.30	*4.43*	*4.01, 3.88*	
X10[a]	8.29	4.50	3.08, 3.08	$C_\delta H$ 7.11, 7.11 $C_\varepsilon H$ 6.80,6.80
	8.45	*4.61*[b]	*2.59, 2.51*[b]	*$C_{11b}H$ 5.60*
X11[a]	8.23	4.23	3.92, 3.84	
		5.32[b]	*3.44, 3.15*[b]	*C_7H 7.57 C_8H 7.14*
				C_9H 7.21 $C_{10}H$ 7.21
				$N_{11}H$ 10.53
R12	8.24	4.09	1.68, 1.68	$C_\gamma H$ 1.38, 1.38 $C_\delta H$ 3.08, 3.08
	8.50	*4.28*	*1.64, 1.64*	*1.41, 1.19 3.00, 3.00*
				$N_\varepsilon H$ 7.19
				7.10
Y13	8.06	4.50	3.09, 2.94	$C_\delta H$ 7.08, 7.08 $C_\varepsilon H$ 6.81, 6.81
	8.17	*4.39*	*2.84, 2.79*	*6.97, 6.97 6.71, 6.71*
R14	8.04	4.10	1.77, 1.70	$C_\gamma H$ 1.57, 1.51 C_δ 3.12, 3.12
	8.20	*4.10*	*1.53, 1.47*	*1.28, 1.05 2.83, 2.70*
				$N_\varepsilon H$ 7.23
				6.90
K15	8.28	4.17	1.80, 1.80	$C_\gamma H$ 1.49, 1.42 $C_\delta H$ 1.67, 1.67
	8.25	*4.16*	*1.71, 1.71*	*1.41, 1.41 1.78, 1.78*
				$C_\varepsilon H$ 2.99, 2.99 $N_\zeta H$ 7.61
				3.00, 3.00 7.61
Q16	8.42	4.24	2.05, 2.05	$C_\gamma H$ 2.37, 2.37 $N_\delta H$ 7.62,6.97
	8.59	*4.29*	*2.05, 1.97*	*2.35, 2.35 7.66, 6.99*
M17	8.41	4.40	2.03, 1.95	$C_\gamma H$ 2.53, 2.43
	8.60	*4.46*	*2.05, 1.98*	*2.61, 2.53*
A18	8.31	4.26	1.37	
	8.50	*4.33*	*1.36*	
V19	8.26	4.04	2.05	$C_\gamma H_3$ 0.93,0.93
	8.34	*4.03*	*2.03*	*0.94, 0.94*
K20	8.43	4.21	1.72, 1.72	$C_\gamma H$ 1.39, 1.30 $C_\delta H$ 1.65, 1.65
	8.53	*4.23*	*1.70, 1.70*	*1.39, 1.31 1.65, 1.65*
				$C_\varepsilon H$ 2.95, 2.95 $N_\zeta H$ 7.61
				2.95, 2.95 7.61
K21	8.36	4.23	1.70, 1.70	$C_\gamma H$ 1.38, 1.30 $C_\delta H$ 1.68,1.68
	8.42	*4.25*	*1.69, 1.69*	*1.37, 1.30 1.67, 1.67*
				$C_\varepsilon H$ 2.98, 2.98 $N_\zeta H$ 7.61
				2.98, 2.98 7.61
Y22	8.39	4.50	2.99, 2.99	$C_\delta H$ 7.11, 7.11 $C_\varepsilon H$ 6.80, 6.80
	8.44	*4.51*	*2.95, 2.95*	*7.09, 7.09 6.79, 6.79*
L23	8.22	4.27	1.55, 1.55	$C_\gamma H$ 1.54 $C_\delta H_3$ 0.90, 0.85
	8.21	*4.28*	*1.52, 1.52*	*1.52 0.90, 0.84*
A24	8.23	4.18	1.38	
	8.27	*4.18*	*1.38*	
A25	8.31	4.30	1.39	
	8.36	*4.26*	*1.36*	
V26	8.21	4.01	2.05	$C_\gamma H_3$ 0.97, 0.97
	8.30	*4.05*	*2.05*	*0.94, 0.94*
L27	8.44	4.31	1.69, 1.57	$C_\gamma H$ 1.64 $C_\delta H_3$ 0.92, 0.86
	8.47	*4.32*	*1.65, 1.56*	*1.65 0.93, 0.86*
$CONH_2$	7.65, 7.18			
	7.67, 7.18			

The underscored values are those whose δ values in PACAP27 and [*S*-IBTM^{10,11}]PACAP27, except for residues 10 and 11, differ more than 0.1 ppm.
[a]X10 and X11 residues are Y10 and S11, respectively, in PACAP and correspond to *S*-IBTM in [*S*-IBTM^{10,11}]-PACAP.
[b]*S*-IBTM C_2H and C_5H protons are equivalent to $C_\alpha H$ protons for residues 10 and 11, and *S*-IBTM $C_{1a}H$,$C_{1b}H$ and $C_{6a}H$,$C_{6b}H$ protons to $C_\beta H$ protons.

Table 2. ^{1}H chemical shifts of PACAP27 and [*S*-IBTM^{10,11}]PACAP27 (in italics) in 30% TFE v/v solution at pH 3.5 and 25 °C (ppm, from TSP)

Residue	NH	$C_\alpha H$	$C_\beta H$	Others
H1		4.39	3.48, 3.44	$C_{\delta 2}H$ 7.46 $C_{\varepsilon 1}H$ 8.68
	4.39	*3.47, 3.44*	*7.45 8.66*	
S2	8.82	4.62	3.95, 3.91	
	8.80	*4.63*	*3.95, 3.91*	
D3	8.72	4.85[a]	2.92, 2.83	
	8.68	*4.83*	*2.88, 2.80*	
G4	8.40	3.98, 3.98		
	8.39	*3.97, 3.97*		
I5	7.90	4.11	1.79	$C_\gamma H$ 1.27, 1.08 $C_\gamma H_3$ 0.77
	7.88	*4.10*	*1.74*	*1.18, 1.01 0.70*
				$C_\delta H_3$ 0.81
				0.76
F6	8.19	4.67	3.25, 3.13	$C_\delta H$ 7.28,7.28 $C_\varepsilon H$ 7.34, 7.34
	8.15	*4.76*	*3.17, 3.07*	*7.25, 7.25 7.28, 7.28*
				$C_\zeta H$ 7.24
				7.25
T7	7.98	4.25	4.34	$C_\gamma H$ 1.28
	7.89	*4.38*	*4.30*	*1.24*
D8	8.41	4.67	2.92, 2.87	
	8.40	*4.78*	*2.90, 2.83*	
S9	8.31	4.24	3.93, 3.93	
	8.38	*4.44*	*4.07, 3.97*	
X10[b]	8.34	4.44	3.10, 3.10	$C_\delta H$ 7.15, 7.15 $C_\varepsilon H$ 6.85, 6.85
	8.78	*4.41*c	*2.67, 2.52*c	*$C_{11b}H$ 5.62*
X11[b]	8.29	4.18	4.08, 4.02	
		5.32[c]	*3.61,3.13*[c]	*C_7H 7.55 C_8H 7.19*
				C_9H 7.23 $C_{10}H$ 7.37
				$N_{11}H$ 10.35
R12	7.99	4.04	1.90, 1.73	$C_\gamma H$ 1.57, 1.57 $C_\delta H$ 3.19, 3.19
	8.54	*4.11*	*1.92, 1.83*	*1.59, 1.50 3.17, 3.17*
				$N_\varepsilon H$ 7.27
				7.16
Y13	8.06	4.34	3.17, 3.17	$C_\delta H$ 7.06, 7.06 $C_\varepsilon H$ 6.84, 6.84
	7.74	*4.34*	*2.88, 2.41*	*6.82,6.82 6.76, 6.76*
R14	8.27	3.83	1.85, 1.85	$C_\gamma H$ 1.70, 1.51 $C_\delta H$ 3.14, 3.14
	7.19	*3.81*	*1.68, 1.53*	*1.40, 1.25 2.99, 2.91*
				$N_\varepsilon H$ 7.20
				7.02
K15	8.03	4.09	1.96, 1.59	$C_\gamma H$ 1.45, 1.45 $C_\delta H$ 1.70, 1.70
	7.80 4.06	*1.88, 1.52*	*1.43, 1.43 1.71, 1.71*	
				$C_\varepsilon H$ 2.93, 2.93 $N_\zeta H$ 7.62
				2.94, 2.94 7.61
Q16	8.16	3.98	2.27, 2.11	$C_\gamma H$ 2.61, 2.35 $N_\delta H$ 7.02, 6.71
	8.30	*3.95*	*2.11, 2.02*	*2.40, 2.34 7.17, 6.74*
M17	8.15	4.23	2.09, 1.98	$C_\gamma H$ 2.43, 2.30
	7.89	*4.23*	*2.07, 2.07*	*2.52, 2.40*
A18	7.92	4.14	1.59	
	7.85	*4.15*	*1.57*	
V19	8.15	3.75	2.22	$C_\gamma H_3$ 1.10, 1.02
	8.04	*3.77*	*2.20*	*1.09, 1.02*
K20	8.16	3.98	1.97, 1.71	$C_\gamma H$ 1.45, 1.45 $C_\delta H$ 1.72,1.72
	8.06	*3.98*	*1.94, 1.71*	*1.46, 1.46 1.71, 1.71*
				$C_\varepsilon H$ 2.97, 2.97 $N_\zeta H$ 7.62
				2.96, 2.96 7.61
K21	8.06	4.04	1.97, 1.61	$C_\gamma H$ 1.45,1.45 $C_\delta H$ 1.71, 1.71
	8.01	*4.05*	*1.96, 1.59*	*1.45, 1.45 1.71, 1.71*
				$C_\varepsilon H$ 2.97, 2.97 $N_\zeta H$ 7.62
				3.00,3.00 7.61
Y22	8.07	4.30	3.28, 3.17	$C_\delta H$ 7.08, 7.08 $C_\varepsilon H$ 6.77, 6.77
	8.06	*4.30*	*3.27, 3.17*	*7.07, 7.07 6.77, 6.77*
L23	8.78	3.96	1.94, 1.46	$C_\gamma H$ 2.01 $C_\delta H_3$ 0.91,0.91
	8.72	*3.98*	*1.95, 1.47*	*2.00 0.92, 0.92*
A24	8.13	4.03	1.51	
	8.12	*4.04*	*1.51*	
A25	7.65	4.19	1.53	
	7.66	*4.20*	1.53	
V26	7.91	3.87	1.98	$C_\gamma H_3$ 0.83, 0.75
	7.91	*3.88*	*2.00*	*0.84, 0.76*
L27	8.26	4.27	1.82, 1.53	$C_\gamma H$ 1.78 $C_\delta H_3$ 0.89, 0.87
	8.26	*4.27*	*1.82, 1.54*	*1.78 0.90,0.88*
$CONH_2$	7.01, 6.91			
		7.02, 6.90		

The underscored values are those whose δ values in PACAP27 and [*S*-IBTM^{10,11}]PACAP27, except for residues 10 and 11, differ more than 0.1 ppm.
[a]Measured at 15 °C.
[b]X10 and X11 residues are Y10 and S11, respectively, in PACAP and correspond to *S*-IBTM in [*S*-IBTM^{10,11}]-PACAP.
[c]*S*-IBTM C_2H and C_5H protons are equivalent to $C_\alpha H$ protons for residues 10 and 11, and *S*-IBTM $C_{1a}H$,$C_{1b}H$ and $C_{6a}H$,$C_{6b}H$ protons to $C_\beta H$ protons.

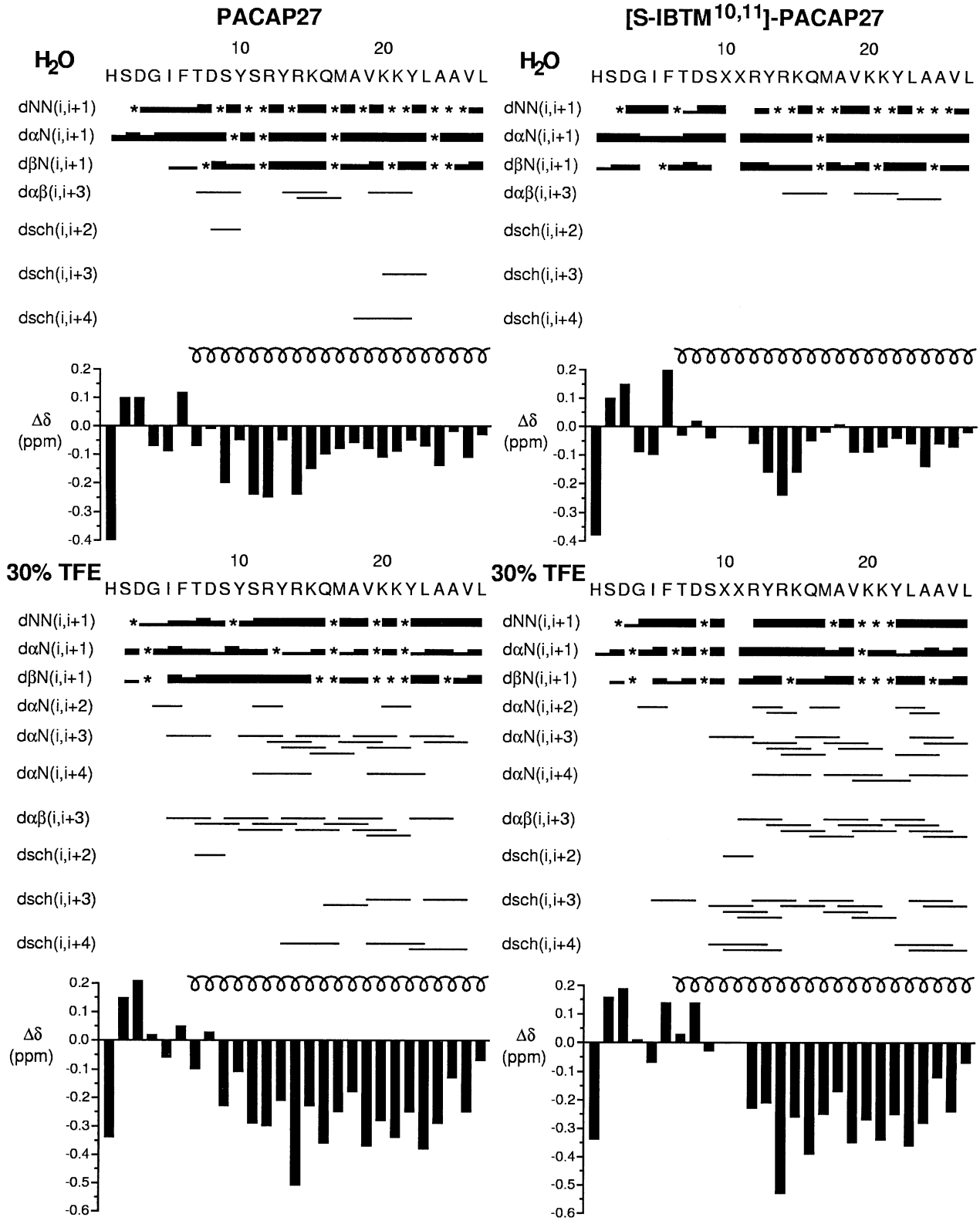

Figure 1. Summary of NOE connectivities and conformational $\Delta\delta_{C\alpha H}$ shifts ($\Delta\delta_{C\alpha H} = \delta_{C\alpha H(observed)} - \delta_{C\alpha H(random\ coil)}$, ppm; where $\delta_{C\alpha H(randomcoil)}$ are the δ corresponding to random coil peptides[51a]) observed for PACAP27 (left) and [*S*-IBTM^{10,11}]-PACAP27 (**1**; right) in aqueous solution (top) and in 30%TFE (bottom) at pH 3.5. The thickness of the lines reflects the intensity of the sequential NOE connectivities, that is, weak, medium, and strong. An asterisk (*) indicates unobserved NOE connectivity due to signal overlapping, closeness to diagonal, or overlapping with solvent signal. NOE conectivities involving side chains are indicated by dsch. The *S*-IBTM^{10,11} peptidomimetic is indicated by XX. *S*-IBTM C_2H and C_5H protons are equivalent to $C_\alpha H$ protons for residues 10 and 11, and *S*-IBTM $C_{1a}H$,$C_{1b}H$ and $C_{6a}H$,$C_{6b}H$ protons to $C_\beta H$ protons.

substantial signal overlap originated by the small signal dispersion and the relatively large size (27 residues) of the peptides. Half of the $d_{\alpha\beta(i,i+3)}$ NOEs expected for the helices adopted by PACAP and [*S*-IBTM^{10,11}]-PACAP27 (**1**) could not be observed because of their overlap with intra-residual NOEs. The experimental data provided no evidence for the β-turn like conformation suggested for PACAP27 by Inooka et al.[21] In aqueous solution at pH 3.5 and 5 °C, the population of helix estimated from the averaged $\Delta\delta_{C\alpha H}$ values within segment T7–L27, as described in the Experimental, was 27% in PACAP27 and 21%, slightly lower, in [*S*-IBTM^{10,11}]-PACAP27 (**1**). The helix length presented by PACAP27 in aqueous solution coincided with that predicted by AGADIR,[35] but the population experimentally found was higher than predicted (15%). A structure calculation for PACAP27 or its analogue **1** in aqueous solution was meaningless due to the small number of non-sequential NOEs identified. Instead, the helices adopted by each peptide were compared, based on the differences in CαH δ values. Assuming differences to be significant when $\Delta\delta > 0.1$ ppm, this analysis revealed substantial changes around residues Y10–S11 and, in general, within the F6–A18 region (Table 1). In brief, the helix adopted by [*S*-IBTM^{10,11}]-PACAP27 (**1**) in aqueous solution appeared to be distorted at the N-terminal region relative to that of the native PACAP27.

More details on the characteristics of the helices formed by PACAP27 and its analogue **1**, and hence, on their differences and similarities, could be derived from the conformational investigation of the two peptides under experimental conditions that favour helix formation. Alcoholic cosolvents are known to increase the helix populations in peptide chains with intrinsic tendency to adopt such structures, though the mechanism of action is unclear.[36] The helix adopted by PACAP27 in aqueous solution (27% of population) was, as expected, less populated than in 50% TFE (60%) and in 25% methanol (46%), estimated by using the δ values reported by Wray et al.,[20] and Inooka et al.,[21] respectively, but it spanned approximately the same residues (S9–T27[20] in 50% TFE at pH 3.0 and 27 °C, and S9–A25[21] in 25% methanol at 30 °C; these helix limits come from a re-evaluation on the basis of the original reported data, NOE and $\delta_{C\alpha H}$ values,[20,21] as in here). Since, according to circular dichroism spectra,[20] PACAP27 reaches its maximum helix content at 30% TFE, we decided to perform an additional NMR study of PACAP27 and its analogue **1** at this relatively low TFE percentage. Combined analysis of the large number of non-sequential, helix-characteristic NOEs, and of $\Delta\delta_{C\alpha H}$ profiles clearly evidences that PACAP27 and its analogue **1** in 30% TFE adopts helix structures that extend approximately over the same residues than in aqueous solution (Figs 1 and 2). Based on the averaged $\Delta\delta_{C\alpha H}$ values within segment T7–L27 (see Experimental), helix populations of 62% for PACAP27 and 56% for [*S*-IBTM^{10,11}]-PACAP27 (**1**) were estimated. Since these helices coexist in equilibrium with random-coil conformations, it is useful to calculate which of them are compatible with the distance constraints derived from the experimental NOEs. Sequential NOEs were excluded from this calculation because of the contribution of random coil conformations to their intensity, except for helix-characteristic $d_{NN(i,i+1)}$ NOEs. For PACAP27 and its analogue **1**, the calculated structures displayed a disordered N-terminal region and a well-defined helix over residues S9–L27. For this helical region, RMSDs for the 20 best-scoring conformers were 0.3 ± 0.1 Å for the backbone atoms and 1.4 ± 0.3 Å for all heavy atoms (including the side chains) in PACAP27, and 0.5 ± 0.2 and 1.4 ± 0.3 Å for the backbone atoms and for all heavy atoms, respectively, in [*S*-IBTM^{10,11}]-PACAP27 (**1**). On the basis of these calculated structures (Fig. 3), we analysed the differences and similarities between the helices adopted by both peptides. The *S*-IBTM framework, designed to fix an H-bond between *n* and *n*+3 residues, displays dihedral angles (49.5, −115.6, −112.6, 26.7°)[25,26] quite different from those of the corresponding residues in the structures calculated for PACAP27 (−76, −28° for Y10; −64, −12° for S11), that are close to those of an ideal α-helix (φ, ψ ca. −60, −40°).[37] The differences in the backbone dihedral angles could be transmitted to the side chains and, therefore, could have a substantial effect on the helix packing. Since most residues within the helix region of PACAP27 and its analogue **1** showed well ordered side chains in the calculated structures (χ_1 angle range $< 30°$), we analysed whether the structures obtained for the two peptides differed in their χ_1 angles. The ordered side chains displayed approximately the same orientation in the two peptides, except for residue R12 (averaged χ_1 angle for the 20 best calculated structures: $-155 \pm 14°$ in PACAP27 and $-92 \pm 8°$ in [*S*-BTM^{10,11}]-PACAP27, **1**).

Binding affinities

The binding affinities of IBTM-containing PACAP27 analogues at PAC_1 and $VPAC_1$ receptors were determined by measuring the displacement of ^{125}I-PACAP27 and ^{125}I-VIP from rat hypothalamus and cerebral cortex homogenates, respectively, as previously described.[38,39] It is known that VIP has a low affinity, in the micromolar range, at PAC_1 receptors, which are abundantly expressed in selected rat brain regions, such as the hypothalamus.[2] ^{125}I-PACAP27 should thereby label predominantly PAC_1 receptors in the latter brain region. In the cerebral cortex, ^{125}I-VIP binds to the $VPAC_1$ receptor, which recognizes VIP and PACAP27/38 with the same high affinity and is abundant in this region.[2] Results are shown in Table 3, in which PACAP6-38, a PACAP fragment with high antagonist potency at PAC_1 receptors, and VIP6-28, an antagonist of VPAC receptors, are also comparatively included.

As shown in Table 3, the conformationally restricted PACAP analogues **1** and **2** bound to PACAP/VIP receptors at concentrations in the micromolar range. The affinity was however higher at $VPAC_1$ receptors, where the affinity of both analogues, as compared to the antagonist VIP6-28, was only 4- to 5-fold lower. The data show that the replacement of the Y10–S11 dipeptide unit of PACAP27 by the IBTM surrogate led to a decrease in binding affinity of 3 orders of magnitude

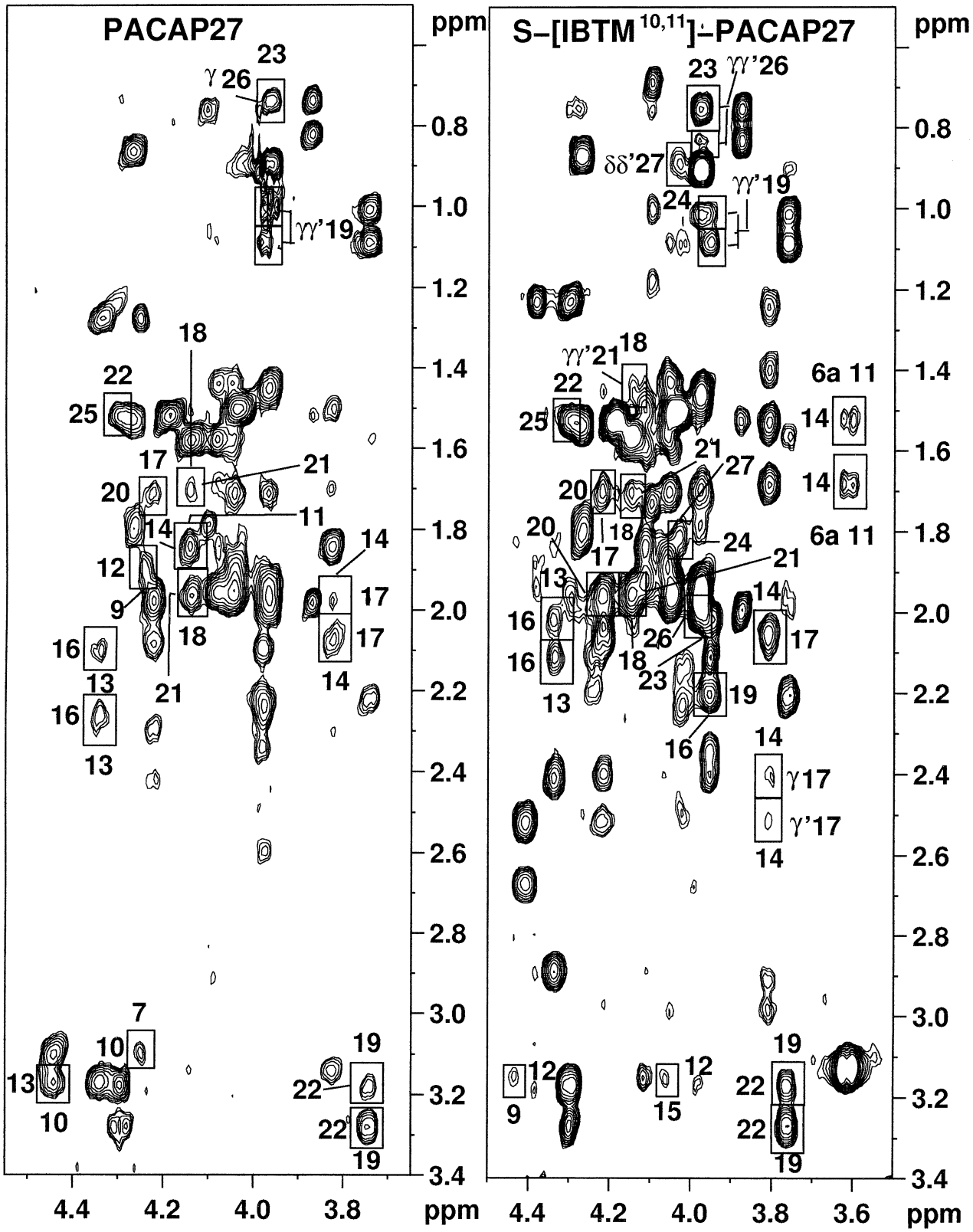

Figure 2. Selected regions of the NOESY spectra of PACAP27 (left) and [*S*-IBTM^{10,11}]PACAP27 (**1**; right) in 30%TFE at pH 3.5 and 25 °C, with a 150 ms mixing time. The non-sequential $d_{\alpha\beta(i,i+3)}$, $d_{\alpha\gamma(i,i+3)}$ and $d_{\alpha\delta(i,i+3)}$ NOEs are boxed and labelled.

relative to the natural peptide (nanomolar range). The detrimental effect of IBTM in compound **1** could be due to the distortion of the global conformation of the neuropeptide, as observed by ^{1}H NMR, which would, in turn, prevent the pharmacophore groups from adopting the bioactive conformation. An alternative explanation could be that the substituted residues, Y10 and S11, are important for receptor recognition. In a recent alanine

scanning in VIP, it has been described that the Y10A mutant resulted in a 20-fold decrease in both the affinity for human $VPAC_1$ receptors and its ability to stimulate adenylyl cyclase activity, while T11 residue can be substituted into alanine without significant alteration of the binding affinity or biological potency.[40] Moreover, three-dimensional structure calculations of these VIP analogues showed that the Y10A mutant, but not the T11A mutant, exhibited a significant change of conformation as compared with native VIP. In addition to that, the role of the H1 residue, which is crucial for the biological activity of VIP, has been explained by specific aromatic interactions with residues F6 and Y10.[41] Although the importance of the individual Y10 residue in PACAP has not been demonstrated yet, it could be predicted that this residue played similar roles in very close peptides, as they are VIP and PACAP. It is worth noting that the binding affinities of PACAP analogue **2**, bearing a type II′ β-turn *R*-IBTM mimetic, are close to those of analogue **1**, with an *S*-IBTM unit able to fix the proposed type II β-turn. This fact suggests that the conformational change of **1** relative to PACAP27 contributes probably less than the lack of the Tyr side chain to the marked decrease in binding affinity. However, a detrimental combination of both factors can not be discarded.

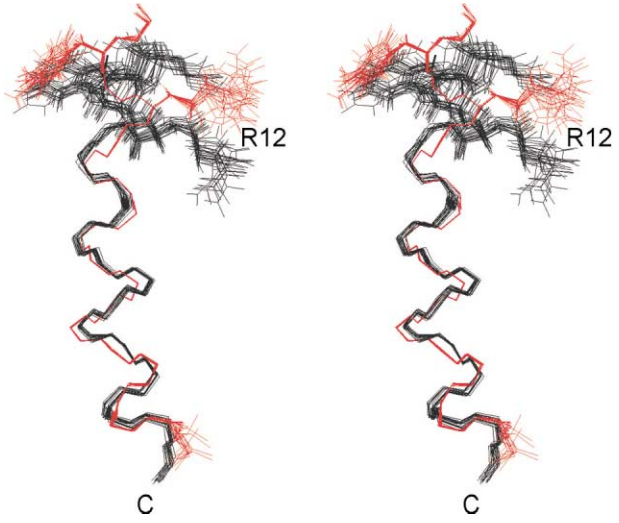

Figure 3. Stereoscopic view of the superposition of backbone atoms (residues 9–27) of the best 20 structures calculated for PACAP27 (red) and [*S*-IBTM^{10,11}]PACAP27 (**1**; black). The side chains of residues 10 (Tyr in PACAP27 and S-IBTM in compound **1**) and 12 (Arg) are also shown. 'C' indicates the C-terminal peptide end.

Table 3. Binding affinities (K_i, nM) of restricted PACAP analogues **1** and **2** at VIP/PACAP receptors

Compd	PAC_1[a]	$VPAC_1$[b]
PACAP27	1.27	1.54
VIP	—	3.10
PACAP6-38	7.1	—
VIP6-28	—	197
[*S*-IBTM^{10,11}]PACAP (**1**)	3104	898
[*R*-IBTM^{10,11}]PACAP (**2**)	5250	1140

Values are the mean of at least three experiments performed in triplicate (standard errors within ±10–15% of the mean).[a]Displacement of ^{125}I-PACAP27 from rat hypotalamus.
[b]Displacement of ^{125}I-VIP from rat cerebral cortex.

Conclusions

To investigate the importance for VIP/PACAP receptor recognition of a proposed β-turn within residues S9–R12 of the PACAP structure, [*S*-IBTM^{10,11}]PACAP27 (**1**) and [*R*-IBTM^{10,11}]PACAP27 (**2**) have been synthesized. *S*-IBTM and *R*-IBTM scaffolds, two proven type II and II′ β-turn mimetics, respectively, were efficiently incorporated into the sequence of PACAP27 by means of SPPS, replacing corner residues Y10–S11. Although it has been reported that PACAP does not adopt defined conformations in aqueous solution,[20] the ^{1}H NMR analysis of PACAP27 and its [*S*-IBTM^{10,11}]PACAP27 analogue **1** in H_2O/D_2O 9:1 suggests otherwise. Thus, based on $C_\alpha H$ conformational shifts and NOE connectivities, PACAP27 showed a disordered N-terminal region of six residues followed by an extended helical region of 21 residues (T7–L27). Contrary to earlier reports,[21] no evidence of a type II β-turn within residues S9–R12 has been found in our conformational study. [*S*-IBTM^{10,11}]PACAP27 (**1**) presented a similar conformational pattern, with an α-helix spanning the T7–L27 region. However, in compound **1**, the α-helix appeared slightly distorted with respect to the native peptide, especially around the IBTM moiety. In the presence of TFE, a known structure-stabilising solvent, the helices adopted by PACAP27 and **1** are more populated, as demonstrated by NOE connectivities and $C_\alpha H$ conformational shifts. Comparison of the structures calculated for the two peptides in 30% trifluoroethanol confirmed that the α-helices formed by PACAP27 and [*S*-IBTM^{10,11}]PACAP27 (**1**) differ at their N-terminal regions, with the side chains of R12 adopting slightly different orientations. In radioligand assays, compounds **1** and **2** showed low affinity for $VPAC_1$, and PAC_1 receptors (μM range), compared to PACAP27 (≈nM). The observed conformational differences between compound **1** and PACAP27 could account, at least in part, for the low affinity of these restricted analogues. However, the lack in **1** of side chains with potential roles in receptor recognition, such as demonstrated for Y10 in VIP,[40] could be a decisive factor for explaining the diminished binding. The incorporation of β-turn mimetics bearing Tyr and Ser side chains, and the evaluation of Y10A and S11A PACAP mutants would be required to know the contribution of these possible factors.

Experimental

Synthesis

Full details on the synthesis and characterization of Boc-*R*- and Boc-*S*-IBTM–OH have appeared previously.[25,42] Solid-phase synthesis of PACAP27 and analogues **1** and **2** was done on *p*-methylbenzhydrylamine resin (0.45 mmol/g), at a 0.1 mmol scale for PACAP and a 0.04 mmol scale for the two analogues. In

situ neutralization protocols[29] and DCC-mediated coupling of Boc-amino acids (4 equivalent each in CH_2Cl_2, 50 min; for Arg and Gln, 4 equivalent amino acid, DCC and HOBt in DMF, 50 min) were used throughout the synthesis, with the following side-chain protecting groups: benzyl (Ser, Thr), benzyloxymethyl (His), 2-bromobenzyloxycarbonyl (Tyr), 2-chlorobenzyloxycarbonyl (Lys), cyclohexyl (Asp) and tosyl (Arg). Activation of the Boc-IBTM pseudodipeptides was done by HATU (4 equivalent each, plus 8 equivalent DIEA, DMF, 90 min). Ninhydrin tests after this first coupling were slightly positive, but negative after recoupling (1.4 equivalent Boc-IBTM and HATU, 2.8 equivalent DIEA, DMF, 90 min). Recouplings, as required by the ninhydrin test, were also performed at other positions, always with DCC-HOBt in DMF. Following sequence assembly, the peptide resins were submitted to low-high HF. The low HF step was done with HF/dimethyl sulfide/*p*-cresol (25:65:10 v/v, 0 °C, 2 h), followed by evaporation and the high HF step with HF/*p*-cresol (90:10, 0 °C, 1 h). The acidolysis crudes were purified by preparative HPLC on C_{18}-silica using a linear 15–35% MeCN gradient in water (both solvents with 0.05% TFA v/v). Fractions judged to be homogeneous by analytical HPLC were pooled and lyophilized. MALDI-TOF MS analysis gave the expected molecular masses [3147.1 for PACAP 27 (monoisotopic MH^+, calcd., 3146.66); 3164.4 Da for [IBTM^{10,11}]PACAP27 (monoisotopic MH^+, calcd. 3163.66)], but also minor peaks at M-18 that were suspected to result from aspartimide formation. Capillary electrophoresis (fused silica, 72 cm×50 μm, 50 cm to detector) in 20 mM sodium citrate at pH 5.2 showed a byproduct eluting ca. 1 min before the main peak, in agreement with the presence of aspartimide. Isoelectric focusing of the HPLC-purified fractions was performed in a Bio-Rad Rotofor system consisting of 20 separation chambers covering the pH range between 0.1 M H_3PO_4 (pH≈2) and 0.1 M NaOH (pH≈13). After focusing for 2 h, the contents of the chambers were collected and reanalyzed by capillary electrophoresis and electrospray MS. For each peptide, an aspartimide-free fraction was identified, lyophilized and desalted by preparative HPLC, as described above.

NMR spectra

Samples for NMR experiments were prepared by disolving the lyophilised peptides in 0.5 mL of H_2O/D_2O (9:1 v/v) or in pure D_2O to a 1–2 mM concentration. pH, measured with a glass micro electrode and uncorrected for isotope effects, was adjusted to 3.5 by addition of minute amounts of DCl or NaOD. The TFE-containing samples were prepared by adding the amount of 2,2,2-trifluoroethanol-d_3 (Cambridge Isotope Laboratories) required to give 30% v/v. The temperature of the NMR probe was calibrated using a methanol sample. Sodium [3-trimethylsilyl 2,2,3,3-^{2}H] propionate (TSP) was used as an internal reference. The ^{1}H NMR spectra were acquired on a Bruker AMX-600 pulse spectrometer operating at a proton frequency of 600.13 MHz. One-dimensional spectra were acquired using 32K data points, which were zero-filled to 64K data points before performing the Fourier transformation. Phase-sensitive two-dimensional correlated spectroscopy (COSY),[43] total correlated spectroscopy (TOCSY),[44] nuclear Overhauser enhancement spectroscopy (NOESY)[45,46] spectra were recorded by standard techniques using presaturation of the water signal and the time-proportional phase incrementation mode.[47] NOESY mixing times were 150 ms. TOCSY spectra were recorded using 80 ms MLEV17 with z filter spin-lock sequence.[44] Data were processed using the standard XWIN-NMR Bruker program on a Silicon Graphics computer. The 2-D data matrix was multiplied by a square-sine-bell window function with the corresponding shift optimised for every spectrum and zero-filled to a 2×1K complex matrix prior to Fourier transformation. Baseline correction was applied in both dimensions.

NMR assignment

The ^{1}H NMR signals of PACAP27 and [*S*-IBTM^{10,11}]-PACAP27 (**1**) in aqueous solution and in 30% TFE were readily assigned by standard methods.[48] For the connection of spin systems through sequential NOE connectivities, IBTM C_2H and C_5H were considered as $C_\alpha H$ protons. ^{1}H δ values of PACAP27 and [*S*-IBTM^{10,11}]-PACAP27 (**1**) in aqueous solution are listed in Table 1 and those in 30% TFE in Table 2.

Estimation of helix populations

The helix populations were quantified on the basis of the $C_\alpha H$ δ values, as previously described.[49] To obtain the helix percentage, the $\Delta\delta_{C\alpha H}$ value [$\Delta\delta_{C\alpha H} = \delta_{C\alpha H(observed)} - \delta_{C\alpha H(random\ coil)}$, ppm] averaged for all the helical residues was divided by the $\Delta\delta_{C\alpha H}$ value corresponding to 100% helix (−0.39 ppm),[50] and then multiplied by 100. The $C_\alpha H$ δ values for non-structured peptides [$\delta_{C\alpha H(random\ coil)}$, ppm] were taken from Wishart et al.[51a] The use of $C_\alpha H$ δ values from other reported sets[51b,c] slightly modifies the absolute values of the estimated populations, but the relative order of the helix populations adopted by PACAP and [*S*-IBTM^{10,11}]-PACAP27 (**1**) remains unchanged.

Structure calculation

Structures were calculated using the program DYANA.[52] The S-IBTM residue was incorporated as a new building-block in the DYANA library with the program MOLMOL.[53] The geometry of this residue was obtained from modelled coordinates.[25] The intensities of the observed NOEs were evaluated qualitatively and translated into upper limit distant constraints: strong (<3.0 Å), medium (<4.0 Å) and weak (<5.0 Å). Pseudo atom corrections were added where necessary, and φ angles were constrained to the range −180° to 0° except for Asn and Gly.

Binding assays

Male Wistar rats (200–220 g) were used throughout.

^{125}I-PACAP27 binding. Binding studies of ^{125}I-PACAP27 to central PACAP receptors were performed

as described[38] with minor modifications. Briefly, the selected brain region was homogenized in 0.25 M ice-cold sucrose, centrifuged at 1000*g* for 10 min at 4 °C and the supernatant was centrifuged again at 20,000*g* for 15 min at 4 °C. The pellet was resuspended in 1 mM $NaHCO_3$ and further diluted in 50 mM Tris–maleate buffer (pH 7.4) containing 2 mM $MgCl_2$, 1% BSA, 100 KIU/ml trasylol and 0.5 mg/mL bacitracin. The incubation mixture contained 70 μL of tissue suspension, 25 μL of ^{125}I-PACAP27 (70 pM final concentration) and 25 μL of incubation buffer containing the test compounds at concentrations from 10^{-11} to 10^{-5} M. Tubes were incubated for 30 min at 37 °C. After rapid filtration through GF/C Whatman filters, presoaked in 0.1% polyethyleneimine, radioactivity was measured in a gamma counter.

^{125}I-VIP binding. Binding of ^{125}I-VIP to VPAC1 receptors in rat cortical homogenates was performed as described.[39] After homogenization of the cerebral cortex in 0.25 M ice-cold sucrose, centrifugation at 1000*g* for 10 min and new centrifugation of the supernatant at 20,000*g* for 30 min at 4 °C, the pellet was suspended in 25 mM Tris–HCl buffer (pH 7.4) containing 2 mM $MgCl_2$, 1 mM β-mercaptoethanol, 1% BSA and 0.5 mg/mL bacitracin. The incubation mixture contained 150 μL of tissue suspension, 25 μL of ^{125}I-VIP (60 pM final concentration) and 25 μL of incubation buffer, containing the test compounds at concentrations from 10^{-11} to 10^{-5} M. Tubes were incubated for 60 min at 37 °C and, after addition of 300 μL of incubation buffer containing 0.25 M sucrose, tubes were centrifuged again at 10,000*g* for 2 min. After washing of the pellet with 300 μL of the latter buffer, radioactivity was measured using a gamma counter.

Acknowledgements

Work at the Instituto de Química Médica and Universidad de Navarra was supported by CICYT (SAF 97 0030 and SAF 2000-0147), Fundación La Caixa (97/022) and Comunidad Autónoma de Madrid (08.5/0006/1998). Work at the Instituto de Estructura de la Materia was supported by DGICYT (PB98-0677) and the European Union (CEE B104-97-2086). Work at the Universidad de Barcelona was supported by Generalitat de Catalunya (CERBA). C.M.S. and M.M.-M. are recipients of a predoctoral and a post-doctoral fellowship, respectively, from the Comunidad Autónoma de Madrid, Spain. E.de O. is a post-doctoral fellow of Fundació Bosch i Gimpera, Universitat de Barcelona, Spain.

References and Notes

1. Vaudry, D.; González, B. J.; Basille, M.; Yon, L.; Fournier, A.; Vaudry, H. *Pharmacol. Rev.* **2000**, *52*, 269.
2. Harmar, A. J.; Arimura, A.; Gozes, I.; Journot, L.; Laburthe, M.; Pisegna, J. R.; Rawlings, S. R.; Robberecht, P.; Said, S. I.; Sreedharan, S. P.; Wank, S. A.; Waschek, J. A. *Pharmacol. Rev.* **1998**, *50*, 265.
3. Christophe, J. *Biochem. Biophys. Acta* **1993**, *1154*, 183.
4. Villalba, M.; Bockaert, J.; Journot, L. *J. Neurosci* **1997**, *17*, 83.
5. Vaudry, D.; Basille, M.; Anouar, Y.; Fournier, A.; Vaudry, H.; Gonzalez, B. J. *Ann. N. Y. Acad. Sci.* **1998**, *865*, 92.
6. Lindholm, D.; Skoglösa, Y.; Takei, N. Ann. *N. Y. Acad. Sci.* **1998**, *865*, 189.
7. Uchida, D.; Arimura, A.; Somogyvari-Vigh, A.; Shioda, S.; Banks, W. *Brain Res.* **1996**, *736*, 280.
8. Takei, N.; Skoglösa, Y.; Lindholm, D. J. *Neurosci. Res.* **1998**, *54*, 698.
9. Said, S. I.; Dickman, K.; Dey, R. D.; Bandyopadhyay, A.; De Stefanis, P.; Raza, S.; Pakbaz, H.; Berisha, H. I. *Ann. N. Y. Acad. Sci.* **1998**, *865*, 226.
10. Shoge, K.; Mishima, H. K.; Saitoh, T.; Ishihara, K.; Tamura, Y.; Shiomi, H.; Sasa, M. *Brain Res.* **1999**, *839*, 66.
11. Gourlet, P.; Vandermeers, A.; Vertongen, P.; Rathe, J.; De Neef, P.; Cnudde, J.; Waelbroeck, M.; Robberecht, P. *Peptides* **1997**, *18*, 1539.
12. Gourlet, P.; De Neef, P.; Cnudde, J.; Waelbroeck, M.; Robberecht, P. *Peptides* **1997**, *18*, 1555.
13. Gourlet, P.; Vandermeers, A.; Vandermeers-Piret, M.-C.; De Neef, P.; Waelbroeck, M.; Robberecht, P. *Biochem. Biophys. Acta* **1996**, *1314*, 267.
14. Xia, M.; Sreedharan, S. P.; Bolin, D. R.; Gaufo, G. O.; Goetzl, E. J. *J. Pharmacol. Exp. Ther.* **1997**, *281*, 629.
15. Gourlet, P.; Vertongen, P.; Vandermeers, A.; Vandermeers-Piret, M.-C.; Rathe, J.; De Neef, P.; Waelbroeck, M.; Robberecht, P. *Peptides* **1997**, *18*, 403.
16. Moro, O.; Lerner, E. A. *J. Biol. Chem.* **1997**, *272*, 966.
17. Moro, O.; Wakita, K.; Ohnuma, M.; Denda, S.; Lerner, e. A. and Tajima, M. *J. Biol. Chem.* **1999**, *274*, 23103.
18. Vandermeers, A.; Vanderborre, S.; Hou, X.; De Neef, P.; Robberecht, P.; Vandermeers-Piret, M.-C.; Christophe, J. *Eur. J. Biochem.* **1992**, *208*, 815.
19. Dickinson, T.; Fleetwood-Walker, S. M.; Mitchell, R.; Lutz, E. M. *Neuropeptides* **1997**, *31*, 175.
20. Wray, V.; Kakoschke, C.; Nokihara, K.; Naruse, S. *Biochemistry* **1993**, *32*, 5832.
21. Inooka, H.; Endo, S.; Kitada, C.; Mizuta, E.; Fujino, M. *Int. J. Pep. Protein Res.* **1992**, *40*, 456.
22. Fry, D. C.; Madison, V. S.; Bolin, D. R.; Greeley, D. N.; Toome, V.; Wegrzynski, B. B. *Biochemistry* **1989**, *28*, 2399.
23. Olson, G. L.; Bolin, D. R.; Bonner, M. R.; Bös, M.; Cook, C. M.; Fry, D. C.; Graves, B. J.; Hatada, M.; Hill, D. E.; Kahn, M.; Madison, V. S.; Rusiecki, V. K.; Sarabu, R.; Sepinwall, J.; Vincent, G. P.; Voss, M. E. *J. Med. Chem.* **1993**, *36*, 3039.
24. De la Figuera, N.; Rozas, I.; García-López, M. T.; González-Muñiz, R. *J. Chem. Soc. Chem. Commun.* **1994**, 613.
25. De la Figuera, N.; Alkorta, I.; García-López, M. T.; Herranz, R.; González-Muñiz, R. *Tetrahedron* **1995**, *51*, 7841.
26. Andreu, D.; Ruiz, S.; Carreño, C.; Alsina, J.; Albericio, F.; Jiménez, M. A.; De la Figuera, N.; Herranz, R.; García-López, M. T.; González-Muñiz, R. *J. Am. Chem. Soc.* **1997**, *119*, 10579.
27. IBTM: 2-amino-3-oxohexahydroindolizino[8,7-b]indole-5-carboxyic acid. For reasons of simplicity, the stereochemistry of the IBTM skeleton is only indicated by the configuration at C11b. Thus, *S*-IBTM: (2*R*,5*R*,11b*S*)-IBTM; *R*-IBTM: (2*S*,5*S*,11b*R*)-IBTM
28. Barany, G.; Merrifield, R.B. In: *The Peptides. Analysis, Synthesis, Biology*. Gross, E., Meienhofer, J., (Eds.), Academic: New York, 1979; pp 1–284
29. Alewood, P.; Alewood, D.; Miranda, L.; Love, S.; Meutermans, W.; Wilson, D. *Method Enzymol.* **1997**, *289*, 14.
30. Carpino, L. A.; El-Faham, A.; Minor, C. A.; Albericio, F. J. *Chem. Soc., Chem. Commun.* **1994**, 201.
31. Tam, J. P.; Heath, W. F.; Merrifield, R. B. *J. Am. Chem. Soc.* **1983**, *105*, 6442.

32. Wishart, D. S.; Sykes, B. D. *Method Enzymol*. **1994**, *239*, 363.
33. Case, D. A.; Dyson, H. J.; Wright, P. E. *Method Enzymol*. **1994**, *239*, 392.
34. Szilágyi, L. *Prog. Nucl. Magn. Reson. Spect*. **1995**, *27*, 325.
35. Muñoz, V.; Serrano, L. *Biopolymers* **1997**, *41*, 495.
36. Buck, M. Q. *Rev. Biophys*. **1998**, *31*, 297.
37. Richardson, J. S.; Richardson, D.C. In *Prediction of Protein Structure and the Principles of Protein Conformation*; Fasman, G. D. (Ed.); Plenum: New York/London 1989; pp 1–98
38. Staun-Olsen, P.; Ottesen, B.; Gammeltoft, S.; Fahrenkrug, J. *Brain Res*. **1985**, *330*, 317.
39. Cauvin, A.; Robberecht, P.; De Neef, P.; Gourlet, P.; Vandermeers, A.; Cristophe, J. *Regul. Pept*. **1991**, *35*, 161.
40. (a) O'Donnell, M.; Garippa, R. J.; O'Neill, N. C.; Bolin, D. R.; Cottrell, J. M. *J. Biol. Chem*. **1991**, *266*, 6389. (b) Nicole, P., Lins, L.; Rouyer-Fessard, C.; Drouot, C.; Fulcrand, P.; Thomas, A.; Couvineau, A., Martinez, J.; Brasseur, R.; Labyrthe, M. *J. Biol. Chem*. **2000**, *275*, 24003.
41. Goossens, J. F.; Cotelle, P.; Chavatte, P.; Henichart, J. P. *Pept. Res*. **1996**, *9*, 322.
42. Martín-Martínez, M.; De la Figuera, N.; Latorre, M.; Herranz, R.; García-López, M. T.; Cenarruzabeitia, E.; Del Río, J.; González-Muñiz, R. *J. Med. Chem*. **2000**, *43*, 3770.
43. Aue, W. P.; Bertholdi, E.; Ernst, R. R. *J. Chem. Phys*. **1976**, *64*, 2229.
44. Rance, M. *J. Magn. Reson* **1987**, *74*, 557.
45. Jeener, J.; Meier, B. H.; Bachmann, P.; Ernst, R. A. *J. Chem. Phys*. **1979**, *71*, 4546.
46. Kumar, A.; Ernst, R. R.; Wüthrich, K. *Biochem. Biophys. Res. Commun*. **1980**, *95*, 1.
47. Redfield, A. G.; Kuntz, S. D. *J. Magn. Reson* **1975**, *19*, 250.
48. Wüthrich, K.; Billeter, M.; Braun, W. *J. Mol. Biol*. **1984**, *180*, 715.
49. (a) Jiménez, M. A.; Bruix, M.; González, C.; Blanco, F. J.; Nieto, J. L.; Herranz, J.; Rico, M. *Eur. J. Biochem*. **1993**, *211*, 569. (b) Jiménez, M. A.; Blanco, F. J.; Rico, M.; Herranz, J.; Nieto, J. L. *Eur. J. Biochem*. **1993**, *211*, 569.
50. Wishart, D. S.; Dykes, B. D.; Richards, F. M. *J. Mol. Biol*. **1991**, *222*, 311.
51. (a) Wishart, D. S.; Bigam, C. G.; Holm, A.; Hodges, R. S.; Sykes, B. D. *J. Biomol. NMR* **1995**, *5*, 67. (c) Merutka, G.; Dyson, H. J.; Wright, P. E. J. *Biomol. NMR* **1995**, *5*, 14.
52. Güntert, P.; Mumentaler, C.; Wüthrich, K. *J. Mol. Biol*. **1997**, *273*, 283.
53. Horadi, R.; Billeter, M.; Wüthrich, K. *J. Mol. Graphics* **1996**, *12*, 29.